

Pressure Loss and Enhancement of Heat Transfer in an Annulus Filled with Aluminum Foam

Joo-Suk Noh, Young Hee Han*, Kye Bock Lee**, Chung Gu Lee*

Department of Air Conditioning & Refrigeration, Kyonggi Institute of Technology, Shihung 429-792, Korea

**School of Mechanical Engineering, Chungbuk National University, Cheongju 361-763, Korea*

Key words: Aluminum foam, Annulus, Non-Darcy flow, Friction factor, Nusselt number

ABSTRACT: An experimental investigation was carried out for 4 different types of the aluminum foam heat sinks which were inserted into the annulus. The purpose of this study is to examine the feasibility of a heat sink with high performance forced convective water cooling in the annulus. The local wall temperature distribution, inlet and outlet pressures and temperatures, and heat transfer coefficients were measured for heat flux of 13.6, 18.9, 25.1, 31.4 kW/m² and Reynolds number ranged from 120 to 9,000.

Experimental results show that the departure from the Darcy's law is evident from the pressure loss and the friction factor is much higher while the significant enhancement in Nusselt number is obtained, and average Nusselt number of aluminum foam with high pore density is much higher than that of aluminum foam with low pore density. Correlations for the friction factor is proposed and used for design of thermal applications.

Nomenclature

A_f : cross section area of annulus [m²]
 A_w : heat transfer area [m²]
 C_E : Ergun's coefficient
 D : diameter of annulus [m]
 Da : Darcy number, K/H^2
 D_h : hydraulic diameter of annulus, $2(r_o - r_i)$ [m]
 dp/dx : pressure gradient
 f : friction factor
 h : heat transfer coefficient [W/m²K]
 K : permeability [m²]
 k : thermal conductivity [W/mK]
 L : length of aluminum foam [m]
 Nu : Nusselt number, hD_h/k_f
 Pr : Prandtl number, $C_p\mu/k$

q : heat flux [kW/m²]
 r : radius of annulus [m]
 Re_d : Reynolds number based on hydraulic diameter number, VD_h/ν
 Re_k : Reynolds number based on permeability, $V\sqrt{K}/\nu$
 T : temperature [K]

Subscripts

d : hydraulic diameter
 f : fluid
 h : hydraulic
 i : inner
 K : permeability
 L : flow direction length on heating part
 m : mean
 o : outer
 x : coordinate of flow direction
 w : wall of annulus

* Corresponding author

Tel.: +82-43-261-3232; fax: +82-43-263-2448

E-mail address: kblee@chungbuk.ac.kr

1. Introduction

The trend towards increasing scales of integration in the IC industry requires a higher level of performance from cooling technology to meet the elevated power dissipation requirement. In the usual commercial fluid-to-fluid heat exchangers, there is an obvious economic incentive to reduce equipment size. This is accomplished by introducing more surface area or augmenting heat transfer coefficients.

Porous media have large contact surfaces with fluids, which enhance heat transfer performance; hence, there are investigations of heat transfer in porous media for many industrial applications such as heat exchangers, the packed-sphere beds, chemical catalytic reactors. A packed bed is frequently utilized in catalytic converters and thermal energy storage devices. One drawback of a packed bed is that it incurs a large pressure drop for the flow, since the packed bed is a dense material of porosity, which implies a void fraction in the material in the range of 0.3~0.6. Foam material has been introduced recently to remedy the above shortcoming. Foam material is a highly permeable porous medium with high porosity, which enables a considerably reduced pressure drop in the flow.

Koh and Stevens⁽¹⁾ found that, for a constant heat flux boundary condition, the wall temperature and the temperature difference between the wall and the coolant can be drastically reduced by the insertion of a high-conductivity steel particles in the channel.

Hwang and Chao⁽²⁾ showed that the forced convective heat transfer coefficient is increased remarkably in the air flow by inserting bronze beads in the channel from the experimental measurements. Kim et al.⁽³⁾ carried out an experimental investigation on the flow and convective heat transfer for the aluminum foam in an asymmetrically heated channel. They showed that the friction factor is much higher at the lower permeable aluminum foams while the

significant enhancement in Nu is obtained.

However, previous studies for the flow characteristics of the porous media appear to be confined to the Darcy flow regime wherein the flow is laminar and inertial forces are negligible and to two basic duct geometries of parallel plates and a circular pipe. Whereas, the effects of a solid boundary or the inertial forces are expected to become more significant near the boundary and in high porosity media, thus causing the application of Darcy's flow to be invalid. However, relatively little attention has been given to the study of these effects.

The present investigation is concerned with the flow through a high porosity medium, with the emphasis on the non-Darcy flow regime. Since the geometry in practical applications would be generally concentric cylinder of annulus, the heat transfer and friction factor measurements in an annulus with porous heat sink were performed for water flow.

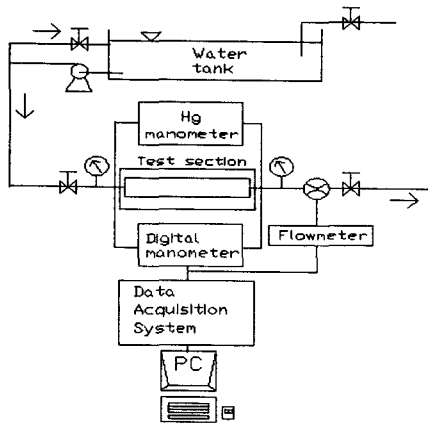
2. Experimental apparatus and test procedure

2.1 Experimental apparatus

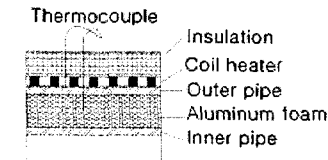
The apparatus employed to study the flow and convective heat transfer characteristics of porous media is represented in Fig. 1. As shown in the figure, it was made up of four major parts: (a) working fluid supply (b) test section (c) porous media and (d) data acquisition system.

The water supplied by the pump from the water tank flows through the copper annulus filled with aluminum foam.

The test section is a flow channel of annulus cross section into which the aluminum foam is inserted and consists of 38.24 mm copper outer tube and 9.52 mm or 15.88 mm copper core tube. The annulus can accommodate hollow shape test specimens of dimension being 38.18 mm OD, 9.54 mm or 15.88 mm ID and length 20~30 mm made by aluminum foams. Figure 2 shows the



(a) Experimental setup



(b) Detail of test section part

Fig. 1 Schematic of experimental apparatus.

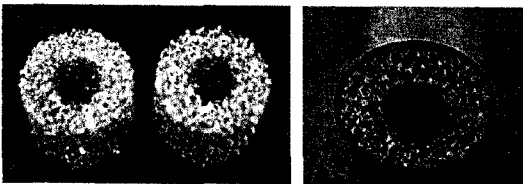


Fig. 2 Aluminum foam and annulus filled with aluminum foam.

aluminum foam and annulus filled with aluminum foam. Electrical coil was covered on the outer tube to provide a constant heat flux condition and the outside of the coil was insulated by thermal ceramics. The power of electrical coil was supplied by the transformer.

The low flow magnetic flow meter (RCM, BadgerMeter, Inc.) was installed to indicate the flow rate at the outlet of test section part. The thermocouple wires were installed on the surface of copper tube wall to measure the local wall temperature. Nine copper constantan thermocouples were axially distributed at 0, 50, 100,

150, 200, 250, 300, 350, and 400 mm from the entrance along the annulus. Three copper constantan thermocouples were vertically distributed at each section to measure the bulk temperature at 0, 100, 200, 300 and 400 mm from the entrance along the annulus. The pressure drop through the test section was measured from the wet digital manometer (Series 490, Dwyer). The temperature readings of the thermocouples were transmitted from the test section to the data acquisition unit (Yokogawa, DA100).

2.2 Test procedure

The test was conducted by increasing the power input ($13.6 \sim 31.4 \text{ kW/m}^2$) to the test section while maintaining a constant flow rate ($0.5 \sim 6 \text{ l/s}$) and a constant inlet temperature of annulus. The corresponding Reynolds number based on the hydraulic diameter (Re_d) ranged from 120 to 9,000 and the Reynolds number based on the permeability (Re_k) ranged from 2 to 150 to cover the operational range for commercial heat exchangers⁽⁴⁾ (non-Darcy flow).

The errors in the temperature measurement were due to the inaccuracies in the initial calibration of the thermocouples and the reading of the recorder. The maximum error was within $\pm 0.1^\circ\text{C}$ for the temperature measurement. The maximum errors both in the flow rate and pressure drop across the test section were less than 1%. An analysis of the general validity of experimental measurements were performed by using an uncertainty analysis.⁽⁵⁾ The uncertainties of the values of Reynolds and Nusselt number by using the root mean square method are within 7.6% and 8.8% in the present experimental study.

3. Results and discussion

3.1 Permeability and friction factor

Table 1 shows the properties of aluminum

Table 1 Flow parameters for aluminum foams

Aluminum foam	A1	A2	B1	B2
Porosity	0.9	0.9	0.9	0.9
Pore density (PPI)	10	20	10	20
Permeability, K (m ²)	7.31×10^{-8}	5.5×10^{-8}	7.28×10^{-8}	3.12×10^{-8}
Ergun coefficient, C_E	0.044909	0.0582882	0.048737	0.060771
Darcy number, K/D_h	8.86×10^{-5}	6.67×10^{-5}	1.46×10^{-4}	6.24×10^{-5}
Radius ratio, r_i/r_o	0.249	0.249	0.415	0.415

foams used in this experiment. For non-Darcy flow with inertial effect in porous media, the axial pressure gradient is represented by the following form.⁽⁴⁾

$$-\frac{dp}{dx} = \frac{\mu}{K} V + \frac{C_E}{\sqrt{K}} \rho V^2 \quad (1)$$

Upon dividing through by μV , Eq. (1) becomes

$$\frac{1}{\mu V} \left(-\frac{dp}{dx} \right) = \frac{1}{K} + \frac{C_E}{\sqrt{K}} \frac{\rho V}{\mu} \quad (2)$$

According to Eq. (2), since K and C_E is constant, the grouping $(-dp/dx)/\mu V$ is a linear function of the grouping $(\rho V/\mu)$. This relationship can be examined from the experimental measurements. Figure 3 has been prepared for this purpose. The grouping $(-dp/dx)/\mu V$ is plotted as the ordinate variable, while $(\rho V/\mu)$ is the abscissa. The dot lines appearing in Fig. 3 are least-square straight lines that have been fitted to the data. The solid line represents the experimental results measured in the channel by Beavers and Sparrow.⁽⁶⁾ In accordance with Eq. (2), the vertical intercepts of the straight line correspond to the values of $1/K$ and the Ergun coefficient is obtained from the slope. The determined permeability K and Ergun coefficient C_E values are represented in Table 1. Figure 3 shows the aluminum foam of high pore density has small permeability for the same radius ratio.

From Eq. (2), we may obtain a general cor-

relation of friction factor f for porous media as follows

$$f = \frac{1}{(\text{Re}_K \text{Da}^{1/2})} + \frac{C_E}{\text{Da}^{1/2}} \quad (3)$$

$$f \text{Da}^{1/2} = \frac{1}{\text{Re}_K} + C_E \quad (4)$$

where

$$f = \frac{\left(\frac{\Delta p}{L} \right) D_h}{\rho V^2}, \quad \text{Da} = \frac{K}{D_h^2}, \quad \text{Re}_K = \frac{\rho V \sqrt{K}}{\mu} \quad (5)$$

To get a correlation of friction factor for aluminum foams, the friction factor data are converted by using non-dimensional groupings $(f \text{Da}^{1/2})$ and (Re_K) as demonstrated in Fig. 4 ($r_i/r_o=0.249$) and Fig. 5 ($r_i/r_o=0.415$).

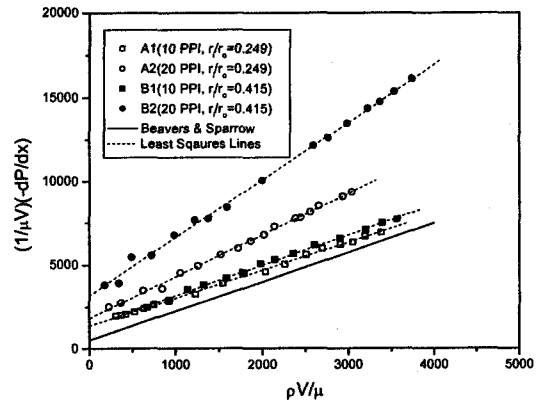


Fig. 3 Relation between axial pressure drop and velocity.

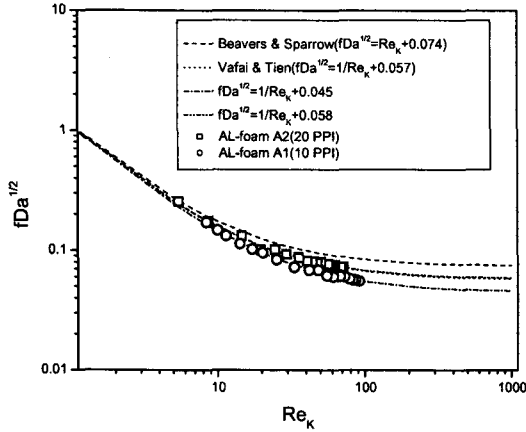


Fig. 4 Relation between friction factor and Reynolds number ($r_i/r_o=0.249$).

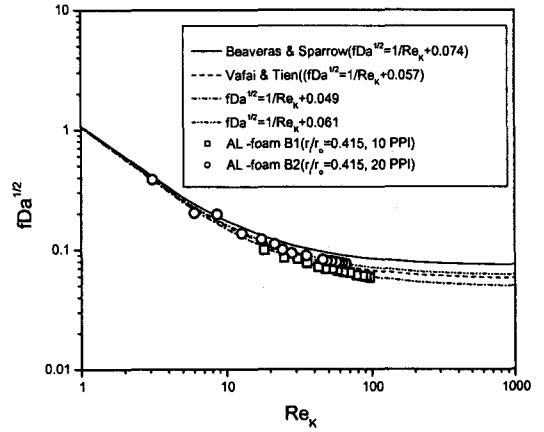


Fig. 5 Relation between friction factor and Reynolds number ($r_i/r_o=0.415$).

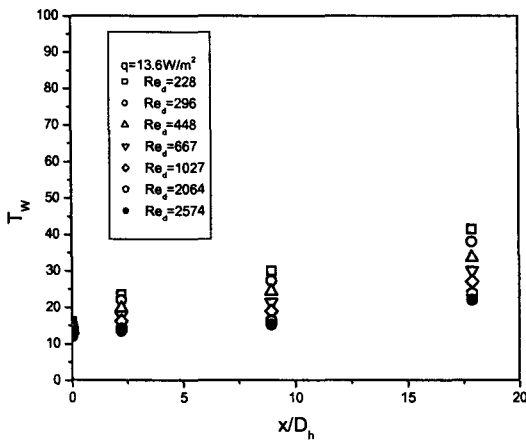
Then, it is found that the present experimental data generally agree to the above correlation Eq. (4). The inertia coefficient C_E varies between 0.045 and 0.061 for the present aluminum foams. The friction factors obtained by Beavers and Sparrow or by Vafai and Tien shows a similar trend.^(6,11)

It can be shown from Figs.4 and 5 that significant departures of the experimental results from Darcy's law first occur at Reynolds numbers on the order of one. At large Reynolds number, departures from Darcy's law are

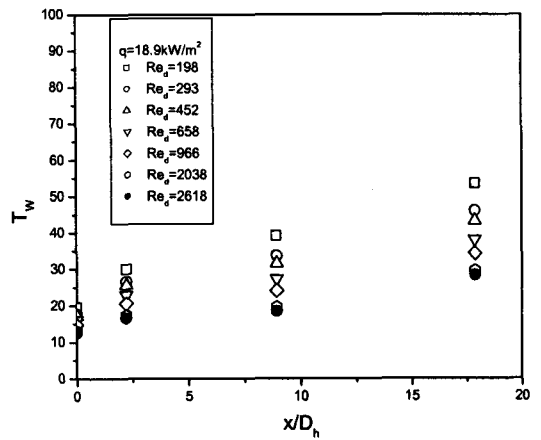
due to inertia effects.

3.2 Nusselt number

Figure 6 shows that the local temperature distribution at four dimensionless axial positions versus Reynolds number for $q=13.6$ and 18.9 kW/m^2 . Higher Re indicates higher mass flow rate applied across the porous channel and causes an increase in the efficiency of the heat exchange between the solid wall and fluid phases. It also shows that the local wall temper-



(a) Heat flux $q=13.6\text{ kW/m}^2$



(b) Heat flux $q=18.9\text{ kW/m}^2$

Fig. 6 Wall temperature distribution as a function of Reynolds number at different axial location.

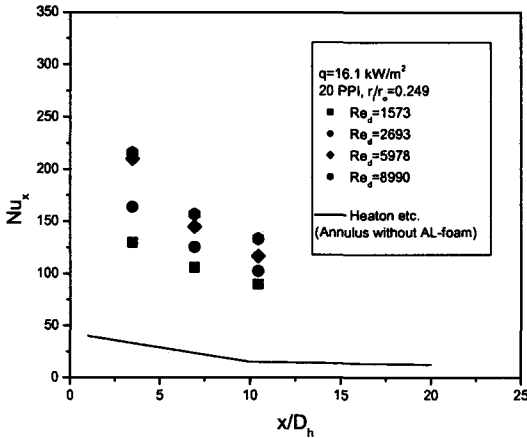


Fig. 7 Local Nusselt numbers for flow through aluminum foams in annulus.

ature increases with the increase in the axial position, x/D_h , the decrease in the Reynolds number and the increase in heat flux q .

To estimate the heat transfer rate of the aluminum foam, the local heat transfer, h_x , and Nusselt number, Nu_x , at a specific location were calculated as

$$Nu_x = \frac{h_x D_h}{k_f} \quad (6)$$

$$h_x = \frac{q}{(T_w - T_{xf})} \quad (7)$$

where q is the heat input unit area, D_h is the hydraulic diameter and k_f is the thermal conductivity of the fluid.

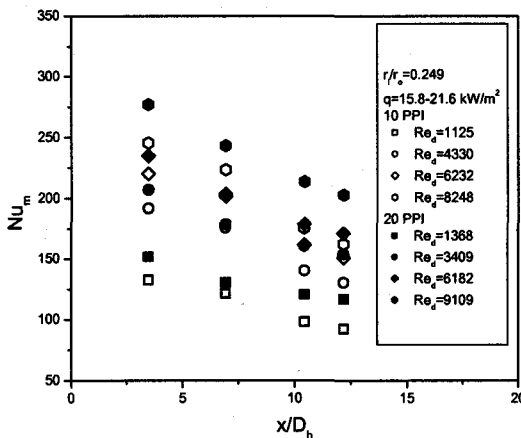
$$q = \frac{\rho C_p V A_f (T_o - T_i)}{A_w} \quad (8)$$

where V is the average velocity, T_i is the inlet temperature, T_o is the outlet temperature and A_f , and A_w are the cross section of the annulus and the heated wall area.

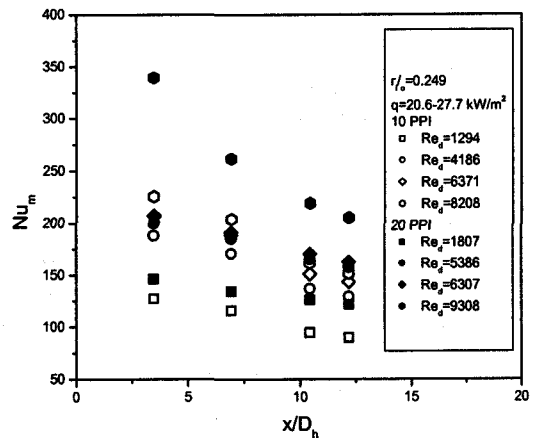
Figure 7 shows the distribution of local Nusselt number as a function of Reynolds number at three dimensionless axial positions. The Nusselt number increases with the increase in the Reynolds number.

The variation of local Nusselt number at all dimensionless axial positions is small at lower Reynolds number. Obviously the thermal entrance length is shorter for small Reynolds number. For an annulus without aluminum foam, the fully developed local Nusselt number was obtained by Heaton et al was plotted in Fig. 7.⁽⁸⁾ Therefore, use of aluminum foam materials as a heat sink causes an increase of the overall heat transfer rates.

The length-averaged heat transfer coefficient is calculated as



(a) Heat flux $q=15.8 \sim 21.6 \text{ kW/m}^2$



(b) Heat flux $q=20.6 \sim 27.7 \text{ kW/m}^2$

Fig. 8 Average Nusselt number for flow through aluminum foams in an annulus.

$$\text{Nu}_m = \frac{h_m D_h}{k_f} \quad (9)$$

$$h_m = \frac{q}{\Delta T_m} \quad (10)$$

$$\frac{1}{\Delta T_m} = \frac{1}{L} \left(\frac{\Delta L_1}{T_{w1} - T_{xf1}} + \frac{\Delta L_2}{T_{w2} - T_{xf2}} + \dots + \frac{\Delta L_n}{T_{wn} - T_{xfn}} \right) \quad (11)$$

Figure 8 presents the average Nusselt number distribution at four dimensionless axial positions versus Reynolds number for radius ratio $r_i/r_o=0.249$. It is seen that the average Nusselt number decreases with the increases in the axial position, x/D_h , the decrease in the Reynolds number. Figure 8 shows that the average Nusselt number of aluminum foam with 10 PPI (Pore Per Inch) is smaller than that of aluminum foam with 20 PPI for the same radius ratio.

4. Conclusions

The present investigation is concerned with the forced convective flow through an annulus filled with aluminum foam involve which is used in heat exchanger. The local wall temperature distribution, inlet and outlet pressure and temperatures, temperatures of fluid between the inlet and outlet were measured to obtain the relationship between flow rate and pressure distribution and heat transfer characteristics.

Experimental results show that the departure from the Darcy's law is evident from the pressure loss and the friction factor is much higher while the significant enhancement in Nusselt number is obtained.

The average Nusselt number of aluminum foam with high pore density is much higher than that of aluminum foam with low pore density. By comparing the experimental data of each type of aluminum foams, correlations for each friction factors are proposed. This technique can be used for the compactness of heat exchanger.

Acknowledgement

This research was supported by the Program for the Training of Graduate Students in Regional Innovation was conducted by the Ministry of Commerce Industry and Energy of the Korean Government.

References

1. Koh, J. C. Y. and Stevens, R. L., 1975, Enhancement of cooling effectiveness by porous materials in coolant passage, *J. of Heat Transfer, Transactions of ASME*, pp.309-311.
2. Hwang, G. J. and Chao, C. H., 1994, Heat transfer measurement and analysis for sintered porous channels, *J. of Heat Transfer, Transactions of ASME*, Vol. 116, pp.456-464.
3. Kim, S. Y., Kang, B. H. and Kim, J. H., 2001, Forced convection from aluminum foam materials in an asymmetrically heated channel, *International J. Heat Mass Transfer* 44, pp. 1451-1454.
4. Kaviany, M., 1995, *Principles of Heat Transfer in Porous Media*, 2nd ed., Springer, p. 48.
5. Kline, S. J. and McClintock, F. A., 1953, Describing uncertainties in single sample experiments, *Mechanical Engineering*, pp.3-8.
6. Beavers, G. S. and Sparrow, E. M., 1969, Non-Darcy flow through fibrous porous media, *J. Applied Mechanics, Transactions of the ASME*, pp. 711-714.
7. Kays, W. M. and Crawford, M. E., 1993, *Convective Heat and Mass Transfer*, McGraw-Hill, Inc., p. 81, 151.
8. Heaton, H. S., Reynolds, W. C. and Kay, W. M., 1964, Heat transfer in annular passages, Simultaneous development of velocity and temperature fields in laminar flow, *Int. J. Heat Mass Transfer*, Vol. 7, pp. 763-781.
9. White, Viscous flow, p.124(Shah and London, *Laminar Flow Forced Convection in Ducts*, 1978, Academic Press).

10. Sparrow, E.M. and Loeffler, J.R., 1959, Longitudinal laminar flow between cylinders arranged in regular array, *AIChE*, Vol. 5, pp. 325-329.
11. Vafai, K. and Tien, C.L., 1980, Boundary and Inertia effects on convective mass transfer in porous media, *Int. J. Heat Mass Transfer*, Vol. 25, No. 8, pp. 1183-1190.